

Cell Reports Medicine, Volume 5

Supplemental information

**A candidate loss-of-function variant
in SGIP1 causes synaptic dysfunction
and recessive parkinsonism**

Marianna Decet, Patrick Scott, Sabine Kuenen, Douja Meftah, Jef Swerts, Carles Calatayud, Sandra F. Gallego, Natalie Kaempf, Eliana Nachman, Roman Prashberger, Nils Schoovaerts, Chris C. Tang, David Eidelberg, Samir Al Adawi, Abdullah Al Asmi, Ramachandiran Nandhagopal, and Patrik Verstreken

Document S1. Supplemental data for Decet et al.

Table S1. Genetic and clinical features of patients with a biallelic mutation in the *SGIP1* gene, related to Figure 1.

| Characteristics | Subject III:1 | Subject III:3 |
|---|----------------------|---|
| Gender | Female | |
| Ethnicity | Arab (Omani) | |
| Inheritance pattern | Autosomal recessive | |
| Chromosome | 1p31.3 | |
| Type of mutation | Homozygous, missense | |
| Exon/intron | Exon 22 | |
| cDNA change | c.2080T>G | |
| Protein change | p.Trp694Gly | |
| Protein domain | Cytoplasmic | |
| Parkinsonism | | |
| Onset age (years) | 19 | 22 |
| Asymmetric onset | Yes | Yes |
| Bradykinesia | Present | Present |
| Rest tremor | Present | Present |
| Rigidity | Present | Present |
| Postural instability | Present | Present |
| Levodopa response | Present | Present |
| Motor fluctuations | Present | Present |
| Dopaminergic drug-induced dyskinesias | Mild | Mild |
| Dopaminergic drug-related worsening of behavioural problems | Present | Present |
| Hoehn-Yahr stage | 4 | 4 |
| Postural tremor | Absent | Present (mild) |
| Seizures (onset age in years) | Absent | Present (Generalised tonic-clonic seizures from age 10) |
| Intellectual and cognitive dysfunction | Present | Present |
| Supranuclear vertical gaze palsy | Absent | Absent |
| Pyramidal signs | Absent | Absent |
| Cerebellar signs | Absent | Absent |
| Autonomic signs | Absent | Absent |
| Bulbar dysfunction | Absent | Absent |
| Brain MRI | Normal | Normal |
| Brain FDG PET (Network analysis): | | |
| PDRP | High | High |
| PDCP | Normal | High |
| MSARP | Low | Low |
| PSPRP | Low | Low |
| Automated differential diagnosis analysis (probability of PD) | 99.5% | 99.7% |

Abbreviations: MRI= magnetic resonance imaging; MSARP= multiple system atrophy related pattern; PET= positron emission tomography; PD= Parkinson disease; PDRP= Parkinson disease-related motor pattern; PDCP= Parkinson disease-related cognitive pattern; PSPRP= progressive supranuclear palsy-related pattern.

Table S2. ROH analyses revealed five homozygous genomic regions shared between the two subjects III:1 and III:3, related to Figure 2.

| Chromosome | Start (bp) | End (bp) | Length (Mb) |
|-------------------|-------------------|-----------------|--------------------|
| Chr1 | 56811604 | 74107645 | 17,3 |
| Chr3 | 78657997 | 90485635 | 11,8 |
| Chr4 | 108120441 | 114552593 | 6,4 |
| Chr5 | 31877748 | 46383335 | 14,5 |
| Chr20 | 7368303 | 12692140 | 5,3 |
| Total | | | 55,4 |

Table S3. *In silico* analysis of pathogenicity prediction of the novel *SGIP1* c.2080T>G (p.W694G) variant, related to Figure 2.

| Prediction Tools | Score (range) | Interpretation |
|-------------------------|-----------------------------|-----------------------|
| phastCons20way | 0.986 | Conserved |
| PhyloP100 | 7.674 (-20 to 30) | Conserved |
| GERP++ | 5.63 | Uncertain |
| SIFT | 0.001 (0 to 1) | Deleterious |
| PolyPhen-2 | 0.976 (0 to 1) | Probably damaging |
| LRT_score | 0 (0 to 1) | Deleterious |
| CADD | 27.5 | Likely deleterious |
| Revel | 0.81 (0 to 1) | Deleterious |
| MUT Assesor | 3 (-5.135 to 6.49) | Supporting |
| FATHMM | -0.45 (-16.13 to 10.64) | Uncertain |
| DANN | 0.98 (0 to 1) | Deleterious |
| MetaLR | 0.48 (0 to 1) | Benign |
| PrimateAI | 0.81 (0 to 1) | Pathogenic |
| BayesDel | 0.364 (-1.29334 to 0.75731) | Moderate Pathogenic |

Figure S1

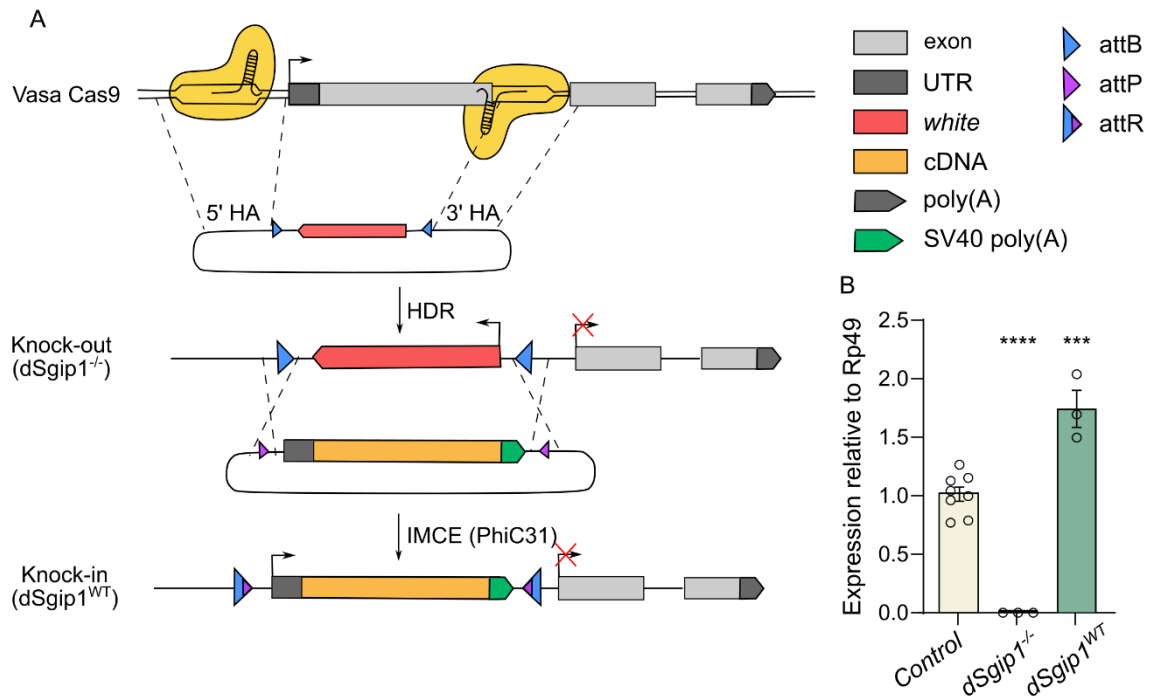


Figure S1. Two-step strategy to generate $dSgip1^{-/-}$ knock-out and $dSgip1^{WT}$ knock-in *Drosophila*, related to Figure 4.

(A) Schematic of the CRISPR/Cas9-based strategy to generate $dSgip1^{-/-}$ knock-out flies. In a second step, the cDNA of $dSgip1^{WT}$ is inserted in the endogenous locus by PhiC31-mediated cassette exchange. HA: homology arm, HDR: Homology directed repair, IMCE: Integrase mediated exchange. See STAR methods. (B) Quantitative RT-PCR to assess $dSGIP1$ mRNA expression levels in adult head extracts relative to Rp49. RT-PCR primers were designed against $dSgip1$. Statistical significance: one-way ANOVA with Dunnett's multiple comparisons test. *** $P < 0.001$, **** $P < 0.0001$. Bars: mean \pm SEM, points are individual values and $n \geq 3$.

Figure S2

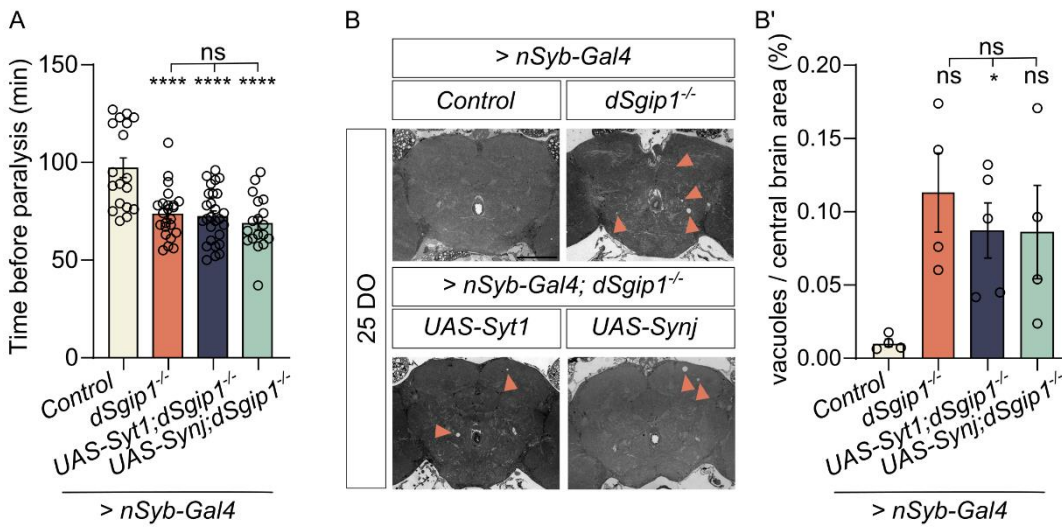


Figure S2. Overexpression of Syt1 and Synj1 do not rescue the paralysis behaviour and degeneration of *dSgip1*^{-/-} mutants, related to Figure 5.

(A) Time (min) before each fly of indicated genotypes shows complete paralysis. Flies were challenged by exposure to 38 °C. Number of tested flies ≥ 18 per genotype, two replicates. Statistical significance: one-way ANOVA. **** P < 0.0001, ns not significant, compared to control. Bars: mean \pm SEM and points are individual values. (B) Widefield images of adult (25 day old) brains of flies of the indicated genotypes stained with toluidine blue. Arrowheads indicate degenerative vacuoles. Scale bar: 100 μ m. (B') Quantification of the area occupied by degenerative vacuoles, expressed as percentage of central brain area. Number of analysed brains ≥ 4 per condition. Statistical significance; Brown-Forsythe and Welch ANOVA tests with a Dunnett's T3 multiple comparisons test. * P < 0.05, ns not significant, compared to control. Bars: mean \pm SEM and points are individual values.

Figure S3

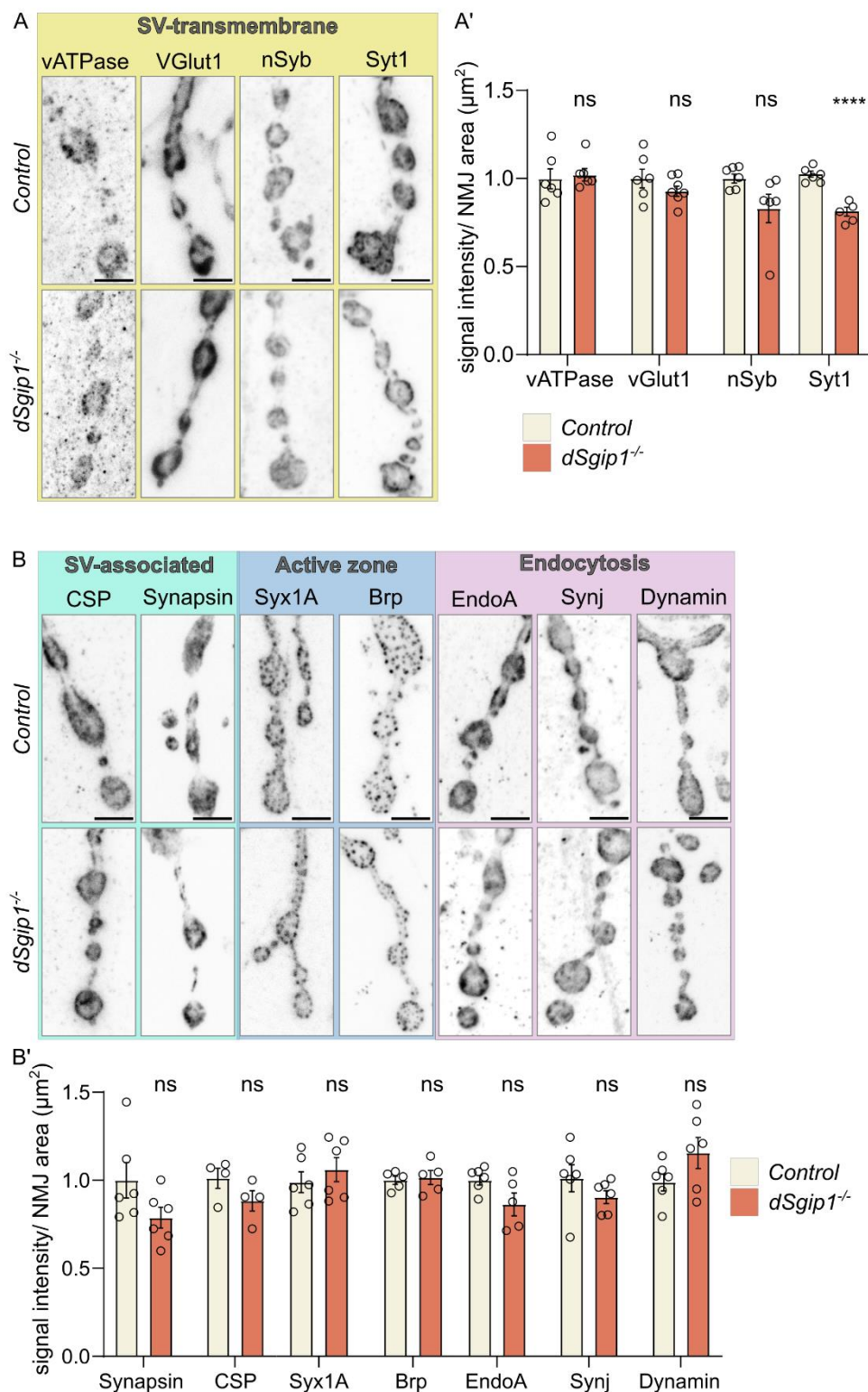


Figure S3. Synaptic protein levels in *dSgip1^{-/-}* mutants, related to Figure 6.

(A-A') Maximum intensity projection confocal images of NMJs of control and *dSgip1^{-/-}* third instar larvae labelled with antibodies against the indicated SV-associated transmembrane proteins (A) and the quantification of the labelling intensity normalized to NMJ area (A'). Scale bar: 5 μ m. (A'). 4 NMJs per animal were quantified, from ≥ 5 animals per condition. Statistical significance: unpaired t-test. Welch's correction applied when the variance

between the two data sets (control and *dSgip1*^{-/-}) was different. **** P < 0.0001, ns not significant. Bars: mean ± SEM and points are individual values. (B-B') Maximum intensity projection confocal images of NMJs of control and *dSgip1*^{-/-} third instar larvae labelled with antibodies against the indicated proteins (B) and the quantification of the labelling intensity levels normalized to NMJ area (B'). Scale bar: 5 μm. 4 NMJs per animal were analysed, from ≥ 5 animals per condition. Statistical significance: unpaired t-test. Welch's correction applied when the variance between the two data sets (control and *dSgip1*^{-/-}) was different. ns not significant. Bars: mean ± SEM and points are individual values.

Figure S4

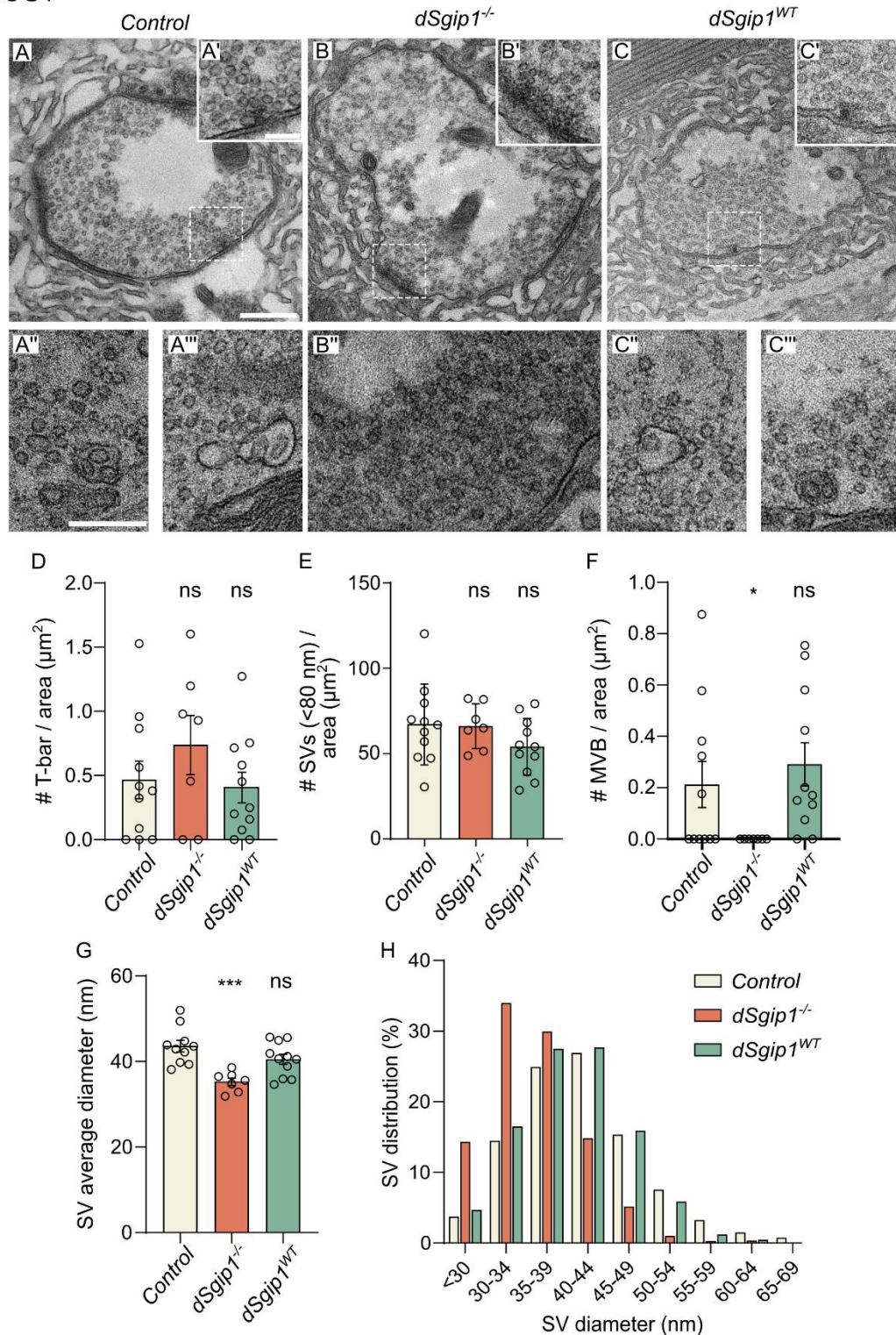


Figure S4. NMJs of *dSgip1^{-/-}* mutants lack multivesicular bodies, related to Figure 7.

(A-C) Transmission electron micrograph (TEM) images of NMJ boutons of third instar larvae of the indicated genotypes. Scale bar: 300 nm. (A'-C') Insets show enlarged areas of indicated active zone areas. Scale bar: 150 nm. (A''-C'' and A'''-C''') TEM images of multivesicular bodies (MVBs) in control (A''-A''') and *dSgip1^{WT}* NMJs (C''-C''') and the lack thereof in *dSgip1^{-/-}* (B''). Scale bar: 250 nm. (D) Quantification of the number of active zones (T-bars) normalized to pre-synaptic bouton area of the indicated genotypes. Statistical significance: unpaired t-

test. ns not significant. Each data point represents a synaptic bouton. Number of animals ≥ 3 per genotype. Bars: mean \pm SEM. (E) Quantification of the number of SVs (< 80 nm) normalized to pre-synaptic bouton area in TEM images of the indicated genotypes. Statistical significance: unpaired t-test. ns not significant. Each data point represents a synaptic bouton. Number of animals ≥ 3 per genotype. Bars: mean \pm SEM. (F) Quantification of the number of multivesicular bodies (MVB) normalized to pre-synaptic bouton area in TEM images of the indicated genotypes. Statistical significance: unpaired t-test: ns not significant, * $P < 0.05$. Each data point represents a synaptic bouton. Number of animals ≥ 3 per genotype. Bars: mean \pm SEM. (G) Quantification of the average diameter of SV (< 80 nm) in TEM images of the indicated genotypes. Statistical significance: unpaired t-test: ns not significant, *** $P < 0.001$. Each data point represents a synaptic bouton. Number of animals ≥ 3 per genotype. Bars: mean \pm SEM. (H) Frequency distribution (in percentage) of the size of SVs (quantified in (G)) plotted in 5 nm bins.